ILL record updated to IN PROCESS
Record 25 of 48

QE 515 C43

ILL pe Record 25 of 48
CAN YOU SUPPLY ? YES NO COND FUTUREDATE
:ILL: 8330683 :Borrower: MFL :ReqDate: 20020709 :NeedBefore: 20020808
:Status: IN PROCESS 20020709 :RecDate: :RenewalReq:
:OCLC: 1553973 :Source: OCLCWEB :DueDate: :NewDueDate:
:Lender: *CLO,CLA,CDS,CFS,CSO
:CALLNO:
:TITLE: Chemical geology.
:IMPRINT: Amsterdam ; New York : Elsevier, 1966-
:ARTICLE: Frantz. "An optical cell for Raman spectroscopic..."
:VOL: 106 :NO: :DATE: 1993 :PAGES: 9-26
:VERIFIED: OCLC ISSN: 0009-2541 [Format: Serial]
:PATRON: STAFF: S. White
:SHIP TO: CSU Moss Landing Marine Labs/Library/8272 Moss Landing Road/Moss Landing, CA 95039
:BILL TO: Same address
:SHIP VIA: ARIEL PREFERRED. 192.190.45.28 :MAXCOST: $15.00
:COPYRT COMPLIANCE: CCL
:FAX: (831)632-4403/Ariel 192.190.45.28
:E-MAIL: parker@mlml.calstate.edu
:BORROWING NOTES: MLML is a part of the California State University System.
:AFFILIATION: IAMSLIC, LVIS, California State University
:LENDING CHARGES: :SHIPPED: :SHIP INSURANCE:
:LENDING RESTRICTIONS:
:LENDING NOTES:
:RETURN TO:
:RETURN VIA:

Chemical Geology, 106 (1993) 9–26
Elsevier Science Publishers B.V., Amsterdam

[EW]

An optical cell for Raman spectroscopic studies of supercritical fluids and its application to the study of water to 500°C and 2000 bar

John D. Frantz[a], Jean Dubessy[a,b] and Bjorn Mysen[a]
[a]*Geophysical Laboratory, Carnegie Institution of Washington, Washington, D.C. 20008, USA*
[b]*CREGU, GS-CNRS 77, F-54501 Vandœuvre-lès-Nancy Cedex, France*

(Received April 16, 1992; revised and accepted November 3, 1992)

ABSTRACT

Frantz, J.D., Dubessy, J. and Mysen, B., 1993. An optical cell for Raman spectroscopic studies of supercritical fluids and its application to the study of water to 500°C and 2000 bar. Chem. Geol., 106: 9–26.

A high-temperature, high-pressure optical cell has been developed for the study of aqueous solutions by Raman spectroscopy. The disk-shaped cell has a sample volume of < 1 ml and utilizes diamond or sapphire windows set at 90° to one-another. Temperatures to 700°C and pressures to 4000 bar have been attained as measured using an internal thermocouple and a strain gauge. The apparatus was employed in the study of water to 500°C and 2000 bar with spectra of the O–H stretching mode being collected at intervals of 50°C and 250 bar. A low-frequency shoulder between 3250 and 3300 cm^{-1} was found to persist to the maximum temperatures to at least 450°C at pressures above those of the liquid vapor curve; its intensity decreased with increasing temperature and decreasing pressure. The frequency of the maximum intensity of the spectral envelope increased dramatically with temperature to above 250°C and was found to be linear with respect to density and independent of temperature at constant density above 250°C. Similar behavior is seen for the viscosity, dielectric constant and the limiting equivalent conductances of pure water. The data indicate the presence of intermolecular hydrogen bonding to temperatures to well above 300°C at densities above the critical density.

1. Introduction

High-temperature, high-pressure fluids are of fundamental importance to heat- and mass-transfer processes in the Earth's crust and mantle. Heat transfer is affected by the flux and heat capacity of intergranular fluids and mass transfer by the processes of mineral dissolution in material transport or mineral precipitation from the fluid. In order to model such processes, the chemical composition, structural speciation and thermodynamics of these intergranular fluids must be known. Electronic and vibrational spectroscopy of aqueous solutions are powerful techniques since they can be used as in situ probes of the structure of electrolytic solutions at high temperatures and pressures. For instance, the structure of water was investigated in pioneering studies using infrared spectroscopy (Frank and Roth, 1967; Valyashko et al., 1980) and Raman spectroscopy (Lindner, 1970; Ratcliffe and Irish, 1982; Kohl et al., 1991). Polyatomic ions give rise to intense Raman spectra and are thus suitable for Raman studies. Dawson et al (1986) used this technique to investigate bisulfate–sulfate equilibria to 300°C. Aqueous complexes can be studied both by UV–visible absorption spec-

Correspondence to: J.D. Frantz, Geophysical Laboratory, Carnegie Institution of Washington, Washington, D.C. 20008, USA.

0009-2541/93/$06.00 © 1993 Elsevier Science Publishers B.V. All rights reserved.

troscopy and Raman spectroscopy depending on the degree of covalency of the bond between the cation and the ligand. UV–visible absorption spectroscopy was used for the characterization of the symmetry of transition elements such as Co and Ni (Ludeman and Franck, 1967, 1968), and more recently for Fe by Susak and Crerar (1985). Non-transition elements such as Pb and Zn were studied by UV absorption spectroscopy (Seward, 1984) and Raman spectroscopy (Irish et al., 1963; Schulz, 1974), respectively. Reviews of these techniques are given by Buback (1981).

Of these spectroscopic techniques, Raman spectroscopy is particularly well suited to the

The optical cell consists of a metal disk [2-in (50.8 mm) diameter×0.75 in (19.1 mm) thick] fabricated from a high-pressure nickel alloy (Stellite®), which contains two holes intersecting at 90° (Fig. 1). Diamonds or synthetic sapphires are fabricated to fit in one end of each hole so that laser illumination can enter the cell and scattered light can be recorded at 90°. The fluid is introduced through one of the other ends of the intersecting holes. The sample cavity contains < 1 ml of fluid.

Sealing of optical windows in high-pressure, high-temperature pressure vessels is critical because of the differences in thermal expansion between the cell and the window material.

lower frequency) at $\nu_1 = 3654\ cm^{-1}$ with associated lower-frequency rotational structures. The infrared spectroscopy of water monomer using matrix isolation techniques in Ar, Kr or N_2 shows the following values: $\nu_1 = 3638$–$3632\ cm^{-1}$ and $\nu_3 = 3734$–$3725\ cm^{-1}$ (Thiel et al., 1957; Tursi and Nixon, 1970; Engdhal and Nelander, 1989). Dimers have been shown to be represented by two distinct Raman bands at 3652 and 3572 cm^{-1} corresponding to the proton acceptor and proton donor molecules, respectively (Buldakova et al., 1986).

The Raman spectrum of liquid water exhibits both intermolecular ($< 1100\ cm^{-1}$) and intramolecular modes ($> 1200\ cm^{-1}$), the former being a characteristic only of liquid water (Walrafen, 1972). Significant differences exist between the intramolecular modes of the liquid and vapor phases. These differences are considerably greater than for other compounds as a result of hydrogen bonding (even compared to dipolar compound such as H_2S). The most striking feature is the existence of the non-symmetric band assigned to the stretching vibrations centered between 3100 and 3900 cm^{-1} with a full width at half maximum (FWHM) of $\sim 400\ cm^{-1}$ at ambient temperature and pressure. This envelope (Fig. 4b) consists of a component near 3250 cm^{-1}, a peak maximum (ν_{max}) around 3400 cm^{-1} and a shoulder at $3625 \pm 10\ cm^{-1}$ (Walrafen et al., 1972, 1986). The band under the low-frequency shoulder (considered for water at room temperature to represent strongly hydrogen-bonded water molecules with local tetrahedral symmetry) lies at a frequency substantially higher than the corresponding band of ice. The wavenumber at the maximum intensity (ν_{max}) at 3425 cm^{-1} is significantly shifted towards lower frequency with respect to ν_1 of the isolated molecule. By contrast, the symmetric stretching frequency of liquid H_2S is 2580 cm^{-1} and of the isolated molecule 2611 cm^{-1} (Herzberg, 1976). The large FWHM of the stretching band points out the importance of intermolecular coupling through hydrogen bonding (Green et al., 1986, 1987; Hare and Sorensen, 1990a, b, 1992). The bending mode of water exhibits a rather weak band around 1636 cm^{-1} (Walrafen, 1972; Brooker et al., 1989; Falk, 1990) and has been shown to be insensitive to pressure and temperature (Ratcliffe and Irish, 1982).

3.2. Experimental results

The principal goal of this study was to investigate the temperature and pressure dependence of the O–H stretching mode of water with the objective of relating the changes in the structure of water under these conditions to changes in its bulk transport properties. The spectra were taken from 2700 to 3900 cm^{-1} using three overlapping spectral windows. Intensities of the overlapping windows were calibrated using a white lamp. Integration times were commonly on the order of 0.5–2 s with

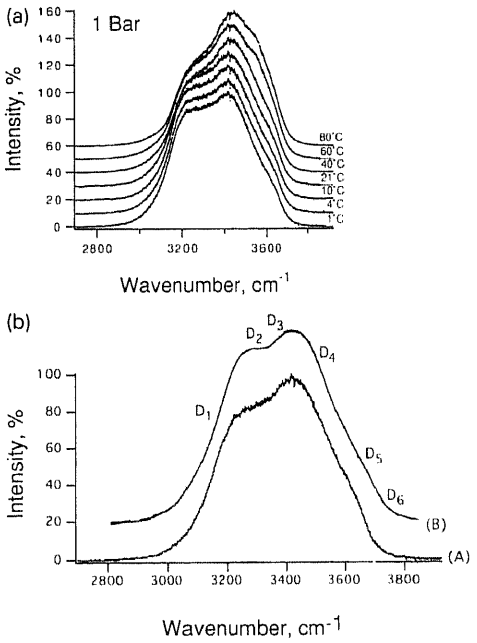

Fig. 4. a. Low-temperature, low-pressure Raman spectra of water using optical cell fitted with water jackets.b. Comparison of water spectra of the present study (*A*) at 1 bar with that of Walrafen et al. (1986) (*B*). Approximate location of inflection points listed in Table 1 are shown as D_i.

100 accumulations. The temperature was raised in increments of 50°C, each being followed by a series of 250-bar pressure increments. All of the data were taken during a single series of measurements on the same fluid sample. As the diamond windows were highly strained, no attempt was made to obtain depolarization ratios. Spectra at temperatures between 1° and 80°C were collected in the previously-described optical cell fitted with water jackets (Fig. 4a). Comparison of the water spectrum collected at 21°C with that of Walrafen et al. (1986) is presented in Fig. 4b. The high-temperature, high-pressure spectra, corrected for temperature and background (Mysen et al., 1982), are shown in Fig. 5. Isobaric sections for 230, 980 and 1990 bar are shown in Fig. 6. Full width at half maximum (FWHM), the frequency of the maximum intensity (ν_{max}), the frequencies of the inflection points (D_i) and the relative intensities (with respect to ν_{max}) of the inflection points (I_{Di}) are given in Table 1. These parameters were determined after computing derivative functions of the spectra. The relative locations of the inflection points are indicated in Fig. 4b. Attempts to deconvolute the whole envelope into three or four bands are difficult because of different shapes for each line.

At 100° and 145°C, the shape of the spectra does not change significantly with pressure. At 100°C, the inflection at 3266 cm^{-1} corre-

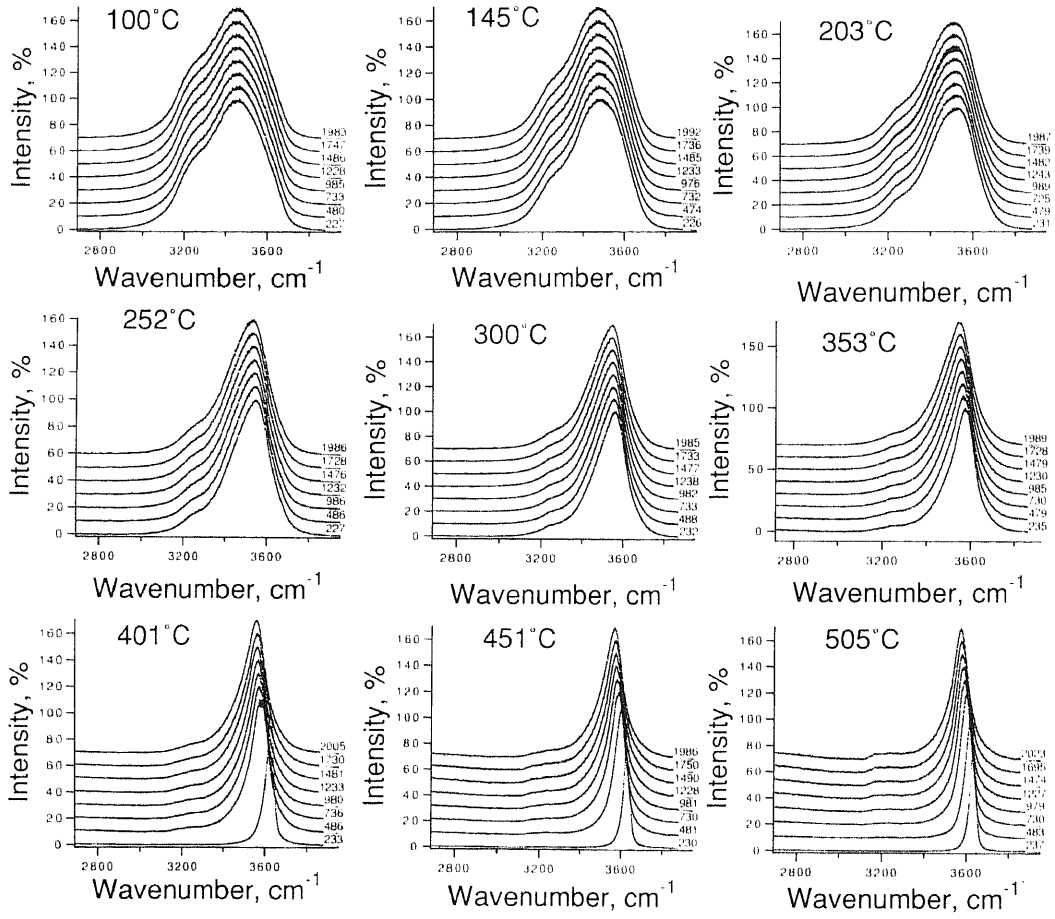

Fig. 5. Isothermal sections of the water spectra corrected for background, frequency and temperature. Individual spectra are labelled with the experimental pressure (bar).

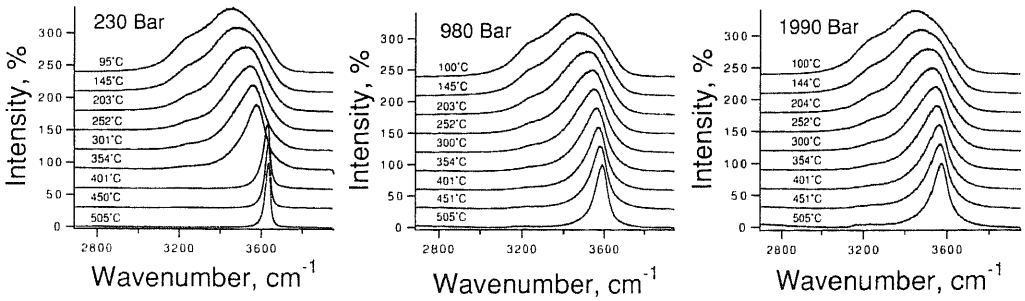

Fig. 6. Isobaric sections of the water spectra.

sponding to the low-frequency shoulder (D_2) has a relative intensity (I_{D2}) of ~60% of the maximum intensity which lies at 3445 cm^{-1}. A high-frequency shoulder is indicated by the inflection points D_5 and D_6. The shape of the peak of the maximum frequency envelope is skewed towards lower frequency. As the temperature increases to 145°C, the relative intensity of the inflection point at 3265 cm^{-1} decreases by 15% with a corresponding decrease in the FWHM. The frequency of maximum intensity (ν_{max}) increases by 30 cm^{-1}.

The spectra taken at 203°C indicate that these same trends continue. The value of I_{D2} indicating the relative intensity of the low-frequency band, has dropped to 30% and the frequency of the maximum intensity (ν_{max}) has substantially increased by as much as 50 cm^{-1} compared with the 145°C spectra. At 203°C, I_{D2} is seen to increase and ν_{max} decreases with increasing pressure. Of particular interest is the increase in the frequency of D_1 as temperature increases from 100° to 203°C. This probably corresponds to a decrease in the contribution of the high-frequency band envelope at lower frequencies as it shifts towards higher frequency. The position of D_2 appears to be independent of temperature. Additionally, due to the frequency shift of the high-frequency envelope, identification of D_5 and D_6 are becoming increasingly difficult. The frequency of D_4 appears to be independent of both temperature and pressure.

The relative intensity of D_2 (I_{D2}) is only 18% at 252°C and the inflection points, D_5 and D_6, can no longer be determined. Because of this, reduced values of FWHM are becoming representative of only the high-frequency portion of the envelope. The shape of the peak of the maximum frequency band envelope is now skewed towards higher frequency whereas at lower temperatures, the skewness is towards lower frequency. The FWHM continues to increase and ν_{max} to decrease with increasing pressure at 252°C.

By 300°C, the frequency of the maximum intensity (ν_{max}) exhibits at constant density a much smaller temperature dependence though the FWHM continues to narrow. Increasing pressure continues to produce the same effects in FWHM and ν_{max} as at lower temperatures. As the contribution of the low-frequency band is small (D_2=9–15%), it is clear that the general shape of the high-frequency band envelope is not symmetric but skewed towards high frequency. The inflection on the high-frequency side of the envelope remains independent of temperature and pressure (Table 1).

Similar trends continue as the temperature increases to 354°, 401°, 451° and 505°C at pressures above the liquid–vapor curve (or the critical isochore: ρ=0.322 g cm^{-3}; Haar et al., 1984). The FWHM continues to narrow with ν_{max} decreasing with increasing pressure but showing little temperature dependence. The low-frequency band continues to persist to 451°C and possibly to 505°C but with very much reduced values of I_{D2}. At pressures below the liquid–vapor curve (or the critical isochore), large changes occur in both ν_{max} and

TABLE 1

Derived parameters of the O–H stretching band envelope

Pressure (bar)	Density (g cm^{-3})	FWHM (cm^{-1})	D_1 (cm^{-1})	D_2 (cm^{-1})	I_{D2} (%)	D_3 (cm^{-1})	ν_{max} (cm^{-1})	D_4 (cm^{-1})	I_{D4} (%)	D_5 (cm^{-1})	D_6 (cm^{-1})
100° C:											
228	0.969	391	3,181	3,267	59	3,382	3,444	3,598	56	3,638	3,630
481	0.977	381	3,180	3,266	57	3,375	3,445	3,598	57	3,616	3,620
734	0.990	394	3,180	3,267	59	3,382	3,446	3,597	59	3,613	3,636
986	0.992	393	3,180	3,266	59	3,382	3,446	3,595	58	3,613	3,642
1,229	1.008	396	3,180	3,266	61	3,381	3,445	3,596	59	3,613	3,644
1,487	1.017	395	3,180	3,267	61	3,383	3,446	3,598	57	3,612	3,639
1,748	1.025	397	3,181	3,274	63	3,383	3,448	3,597	56	3,613	3,643
1,984	1.033	398	3,181	3,284	61	3,383	3,445	3,597	57	3,613	3,645
145° C:											
227	0.934	324	3,189	3,266	44	3,375	3,476	3,598	66	3,614	3,641
475	0.946	320	3,184	3,270	45	3,383	3,477	3,596	66	3,613	3,637
733	0.957	330	3,192	3,266	46	3,383	3,475	3,600	63	3,613	3,649
977	0.968	331	3,189	3,265	46	3,381	3,475	3,596	65	3,614	3,635
1,234	0.978	331	3,181	3,265	47	3,384	3,475	3,596	65	3,613	3,643
1,486	0.987	339	3,181	3,267	48	3,383	3,476	3,597	63	3,613	3,637
1,737	0.996	338	3,191	3,266	47	3,383	3,474	3,598	62	3,617	3,643
1,993	1.006	346	3,183	3,251	46	3,381	3,473	3,607	57	3,613	3,644
203° C:											
232	0.877	261	3,214	3,266	28	3,424	3,527	3,597	70	3,614	3,642
480	0.893	264	3,216	3,265	30	3,423	3,526	3,595	72	3,613	3,649
726	0.907	264	3,213	3,267	30	3,423	3,519	3,596	70	n.a.	n.a.
990	0.921	264	3,214	3,263	30	3,422	3,519	3,597	67	n.a.	n.a.
1,244	0.932	269	3,214	3,264	31	3,423	3,511	3,595	69	n.a.	n.a.
1,483	0.943	266	3,216	3,265	32	3,424	3,519	3,595	68	n.a.	n.a.
1,740	0.953	266	3,207	3,267	32	3,424	3,508	3,596	65	3,614	3,635
1,988	0.963	272	3,213	3,280	35	3,424	3,507	3,590	70	3,613	3,625
252° C:											
228	0.816	215	3,217	3,278	18	3,440	3,544	3,597	73	3,613	3,628
487	0.839	218	3,215	3,264	18	3,441	3,542	3,597	72	n.a.	n.a.
987	0.874	224	3,215	3,265	20	3,424	3,541	3,597	70	n.a.	n.a.
1,233	0.887	224	3,214	3,265	20	3,424	3,537	3,596	69	n.a.	n.a.
1,477	0.900	227	3,213	3,266	21	3,422	3,534	3,588	75	n.a.	n.a.
1,729	0.914	230	3,213	3,278	23	3,424	3,524	3,594	69	n.a.	n.a.
1,987	0.925	231	3,209	3,264	22	3,422	3,531	3,597	65	n.a.	n.a.
300° C:											
233	0.739	174	3,216	3,258	9	3,529	3,560	3,597	76	n.a.	n.a.
489	0.775	178	3,216	3,274	11	3,515	3,550	3,596	75	n.a.	n.a.
734	0.801	180	3,214	3,269	12	3,490	3,544	3,597	71	n.a.	n.a.
983	0.822	187	3,213	3,262	13	3,490	3,547	3,595	72	n.a.	n.a.
1,239	0.841	190	3,219	3,267	14	3,472	3,544	3,597	68	n.a.	n.a.
1,478	0.856	192	3,217	3,264	14	3,490	3,543	3,597	67	n.a.	n.a.
1,734	0.871	195	3,212	3,262	15	3,480	3,542	3,597	65	n.a.	n.a.
1,986	0.885	196	3,214	3,266	15	3,454	3,542	3,597	66	n.a.	n.a.

TABLE 1 (*continued*)

Pressure (bar)	Density (g cm^{-3})	FWHM (cm^{-1})	D_1 (cm^{-1})	D_2 (cm^{-1})	I_{D2} (%)	D_3 (cm^{-1})	ν_{max} (cm^{-1})	D_4 (cm^{-1})	I_{D4} (%)	D_5 (cm^{-1})	D_6 (cm^{-1})
351°C:											
109	0.050	29	n.a.	n.a.	n.a.	3,632	3,640	3,647	66	n.a.	n.a.
354°C:											
236	0.605	125	3,217	3,263	3	3,532	3,575	3,609	69	n.a.	n.a.
480	0.684	136	3,212	3,262	5	3,527	3,564	3,596	79	n.a.	n.a.
731	0.726	143	3,214	3,259	6	3,528	3,564	3,598	73	n.a.	n.a.
986	0.755	149	3,213	3,267	7	3,528	3,564	3,595	74	n.a.	n.a.
1,231	0.780	153	3,212	3,263	8	3,528	3,556	3,598	68	n.a.	n.a.
1,480	0.801	156	3,216	3,266	9	3,517	3,553	3,596	68	n.a.	n.a.
1,729	0.819	158	3,214	3,263	9	3,514	3,550	3,594	70	n.a.	n.a.
1,990	0.836	162	3,214	3,271	10	3,515	3,547	3,595	67	n.a.	n.a.
376°C:											
200	0.128	43	n.a.	n.a.	n.a.	3,618	3,628	3,637	83	n.a.	n.a.
207	0.143	49	n.a.	n.a.	n.a.	3,616	3,626	3,640	65	n.a.	n.a.
215	0.167	55	n.a.	n.a.	n.a.	3,614	3,626	3,639	68	n.a.	n.a.
222	0.207	64	n.a.	n.a.	n.a.	3,613	3,620	3,636	75	n.a.	n.a.
228	0.404	82	n.a.	n.a.	n.a.	3,587	3,610	3,635	70	n.a.	n.a.
236	0.460	94	n.a.	n.a.	n.a.	3,567	3,594	3,627	63	n.a.	n.a.
232	0.440	94	n.a.	n.a.	n.a.	3,567	3,594	3,628	63	n.a.	n.a.
242	0.479	97	n.a.	n.a.	n.a.	3,556	3,589	3,619	72	n.a.	n.a.
401°C:											
234	0.138	41	n.a.	n.a.	n.a.	3,615	3,628	3,640	69	n.a.	n.a.
487	0.565	104	3,214	3,268	2	3,561	3,581	3,604	29	n.a.	n.a.
737	0.645	114	3,224	3,267	3	3,540	3,573	3,599	77	n.a.	n.a.
981	0.688	117	3,218	3,266	4	3,527	3,570	3,597	75	n.a.	n.a.
1,234	0.722	124	3,212	3,267	5	3,528	3,567	3,597	72	n.a.	n.a.
1,731	0.771	130	3,212	3,262	5	3,528	3,563	3,595	72	n.a.	n.a.
2,006	0.792	135	3,223	3,266	6	3,528	3,558	3,596	67	n.a.	n.a.
451°C:											
231	0.097	32	n.a.	n.a.	n.a.	3,624	3,632	3,643	60	n.a.	n.a.
482	0.379	72	n.a.	n.a.	n.a.	3,581	3,603	3,625	64	n.a.	n.a.
731	0.538	88	n.a.	n.a.	n.a.	3,561	3,586	3,609	72	n.a.	n.a.
982	0.471	95	3,213	3,265	1	3,555	3,576	3,597	81	n.a.	n.a.
1,229	0.653	103	3,212	3,265	2	3,539	3,571	3,597	76	n.a.	n.a.
1,491	0.689	109	3,214	3,267	1	3,540	3,570	3,597	71	n.a.	n.a.
1,751	0.718	115	3,213	3,265	2	3,529	3,569	3,598	70	n.a.	n.a.
1,987	0.740	118	3,218	3,267	3	3,527	3,5p64	3,595	69	n.a.	n.a.
505°C:											
238	0.083	30	n.a.	n.a.	n.a.	3,623	3,633	3,642	68	n.a.	n.a.
484	0.236	47	n.a.	n.a.	n.a.	3,605	3,617	3,630	69	n.a.	n.a.
731	0.412	67	n.a.	n.a.	n.a.	3,581	3,599	3,622	62	n.a.	n.a.
980	0.514	74	n.a.	n.a.	n.a.	3,563	3,588	3,609	69	n.a.	n.a.
1,228	0.575	80	n.a.	n.a.	n.a.	3,562	3,584	3,609	61	n.a.	n.a.
1,475	0.620	84	n.a.	n.a.	n.a.	3,555	3,576	3,597	76	n.a.	n.a.
1,696	0.651	87	n.a.	n.a.	n.a.	3,547	3,573	3,599	68	n.a.	n.a.
2,024	0.689	90	n.a.	n.a.	n.a.	3,540	3,570	3,596	68	n.a.	n.a.

n.a. indicates that the position or relative intensity of the derivative was not measureable.

FWHM. The Raman spectrum of water vapor was recorded at 351°C and 109 bar (Fig. 7). It exhibits a single band with ν_{max} being 3640 cm^{-1}, a value considerably higher than that found for the liquid densities and close to the frequency of the isolated water molecule ($\nu_1 = 3656.65$ cm^{-1}). Its FWHM is also considerably reduced compared to liquid (29 vs. 125 cm^{-1} at 109 and 236 bar, respectively). The shape of the band is asymmetric and the shoulder around 3250 cm^{-1} has completely vanished. A series of spectra was recorded at 376°C, close to the critical temperature ($T_c = 373.976$°C; Haar et al., 1984) over a small pressure interval (200–242 bar) to document the spectral changes from water vapor to liquid-like water (Fig. 8). The spectra clearly show a rapid change of both ν_{max} and FWHM. The value of FWHM monitors the change from vapor density to liquid density which occurs between 222 and 228 bar whereas the greatest

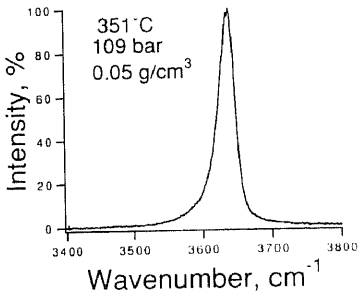

Fig. 7. Raman spectra of water at 351°C and 109 bar (density = 0.05 g cm^{-3}).

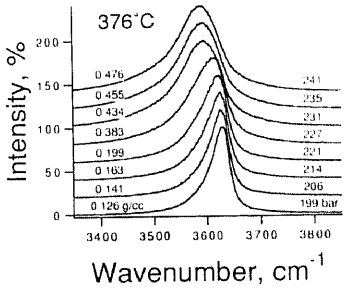

Fig. 8. Isothermal section of water at low pressures near the critical density at 376°C. Individual spectra are labelled with both the density and the experimental pressure (bar).

shift in ν_{max} occurs in the liquid density range between 227 and 236 bar. As the temperature increases from 401° to 451° to 505°C, the pressure range over which this dramatic spectral change occurs increases. There is a distinct correlation between changes in the normally constant D_4 and the large variation in FWHM associated with this transition.

3.3. Density correlations and bulk transport properties

The water spectra as shown in Figs. 5 and 6 indicate significant spectral dependence on both temperature and pressure. An alternative and perhaps more meaningful set of parameters by which the spectra can be described are temperature and density. As the latter is proportional to the number of molecules per unit volume, the effect of temperature as a function of average intermolecular distances can be investigated. Sets of spectra corresponding to densities of (a) 0.92–0.93 g cm^{-3}; (b) 0.87–0.88 g cm^{-3}; (c) 0.77–0.78 g cm^{-3}; and (d) 0.69 g cm^{-3} are presented in Fig. 9. Densities are obtained from Haar et al. (1984). The spectra in Fig. 9a and b show clearly that O–H oscillators at similar average intermolecular distances display varying energy distributions as a function of temperature. For density of 0.92–0.93 g cm^{-3}, ν_{max} shifts towards higher frequency (145°C: 3476 cm^{-1}; 203°C: 3511 cm^{-1}; 252°C: 3531 cm^{-1}), FWHM decreases (145°C: 320 cm^{-1}; 203°C: 269 cm^{-1}; 252°C: 231 cm^{-1}) and I_{D2} decreases (145°C: 44%; 203°C: 31%; 252°C: 22%). Similar trends were observed in the early work of Lindner (1970) for a density of 1.0 g cm^{-3} at temperatures up to 400°C and pressures to 5000 bar. Isochoric sections at lower density shown in Fig. 9c and d illustrate a somewhat different behaviour: ν_{max} varies little as a function of temperature. However, FWHM and I_{D2} continue to remain sensitive to changes in temperature: for the 0.77–0.78 g cm^{-3} isochoric section, FWHM- and I_{D2}-values respectively are 178 cm^{-1} and

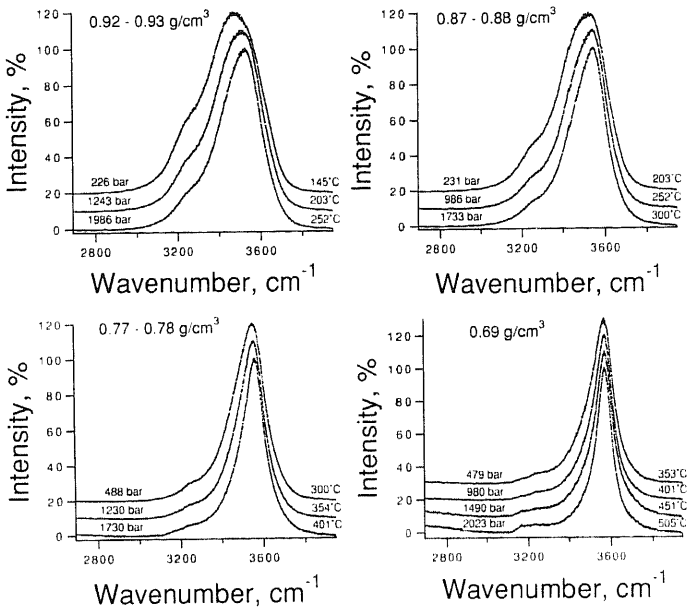

Fig. 9. Isochoric sections of water spectra.

11% at 300°C; 153 cm^{-1} and 8% at 354°C; 130 cm^{-1} and 5% at 400°C.

As noted in examination of Table 1 and the isochoric sections in Fig. 9, the fundamental parameter influencing ν_{max} below 250°C is temperature; at temperatures above 250°C, density becomes the dominant parameter. This behavior is shown in Fig. 10a in which the values of ν_{max} measured from all of the spectra collected in this study are plotted as a function of their corresponding densities. The data include both liquid-like and vapor-like fluids. At temperatures over 250°C, the value of ν_{max} is approximately linear with respect to density and independent of temperature at any particular density (including both liquid-like and vapor-like densities). Distance between molecules rather than thermal energy becomes fundamental. ν_{max} remains a linear function of density down to 0.1 g cm^{-3}. At temperatures higher than 250°C, these trends strongly suggest the presence of a dominant high-frequency band representing a single dominant inter-/intramolecular coupling of O–H oscillators. In addition, due to the large dependence of the frequency of this band on density, it can be inferred that dipole–dipole interactions (or possibly transient hydrogen bonding) remain important in molecular O–H vibrations to the lowest densities and highest temperatures of this study. The data point recorded at 351°C for a 0.05 g cm^{-3} density significantly departs from this linear trend and produces an inflection point which makes our data consistent with the low-density frequency vibration of isolated water molecules at 3656.7 cm^{-1}. This feature documents rather strong molecular interactions even in the vapor phase as it is also indicated by the value of the second virial coefficient of the vapor water (Whalley et al., 1991).

At temperatures below 300°C, the spectral envelope in the vicinity of ν_{max} indicates the presence of at least two (if not more) bands. The O–H oscillators responding to other molecular environment(s) have become much more important than at higher temperatures where they appear to play a minor role. As shown in Fig. 5 and described in the previous section, the shape of the peak is skewed towards higher frequency at 300°C and reflects the skewness of this portion of the envelope as

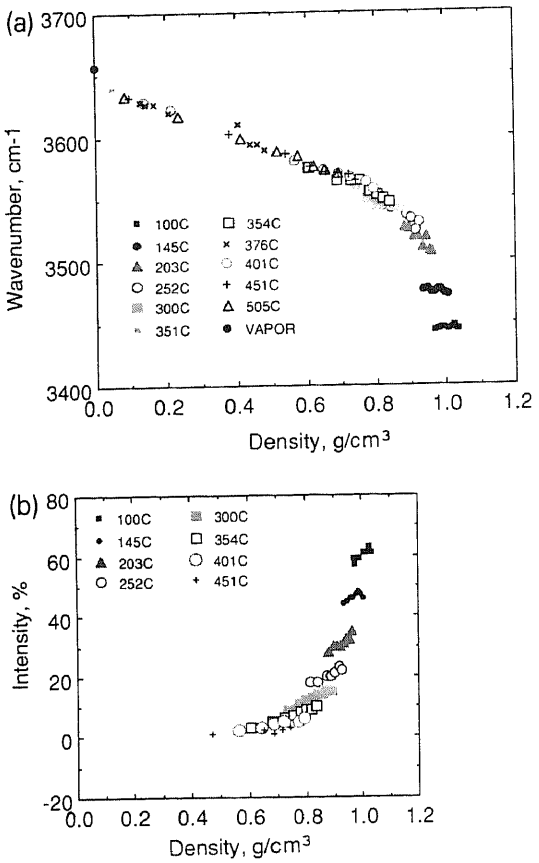

Fig. 10. a. The frequency of the envelope maximum (ν_{max}) as a function of density and temperature.b. The intensity of the inflection point D_2 as a function of density and temperature.

a whole. As the temperature is progressively decreased, the skewness disappears and then reappears towards lower frequency as the temperature approaches 100°C. These trends, combined with the observation that the inflection (D_4) on the high-frequency side of ν_{max} is insensitive to temperature and density changes at the low temperatures (Table 1), indicate that the band represented by the linear relationship between frequency and density in Fig. 10 persists (though is no longer dominant) to the lowest temperatures of this study.

While the frequency of the maximum of the envelope (ν_{max}) is very sensitive to temperature between 100° and 300°C, similar frequency shifts do not occur in the case of the low-frequency shoulder. For densities above the critical density, the inflection point (D_2) remains constant at ~ 3265 cm^{-1} with increasing pressure and decreasing density to at least 451°C. However, the relative intensity of the inflection point (I_{D2}) decreases with increasing temperature and decreasing density (Fig. 10b). This temperature dependence of I_{D2} extends above 400°C until it can no longer be measured. As the frequency of this band remains constant above critical densities, this indicates that the OH oscillators experience a perturbation, by surrounding molecules, which depends on the mean average distance between water molecules but which is temperature independent. This feature suggests that the band under this shoulder represents vibrations in "tetrahedral" clusters of hydrogen-bonded water molecules. In a first approximation, the frequency of O–H oscillators in such clusters would be insensitive to the average intermolecular distances between molecules; they would primarily be sensitive to the intermolecular distances between molecules only within the clusters themselves.

The behavior of the bulk transport properties of water as functions of temperature and density parallel the observed spectral trends. In Fig. 11a, the viscosity (Haar et al., 1984) is plotted as a function of density and temperature for all the temperature–density combinations of the spectral study. The viscosity is seen to be highly temperature dependent to 250°C. At temperatures above this value, the viscosity becomes an almost linear function of density and is temperature independent at constant density. The trends shown in Fig. 11a are intriguingly similar to those of Fig. 10a. At the lower temperatures of the present study (<250°C), hydrogen bonding appears to result in a substantial portion, if not most, of the water molecules being in some way structurally associated with one another. As stated above, the band at ~ 3265 cm^{-1} in all probability indicates clusters of hydrogen bonded molecules;

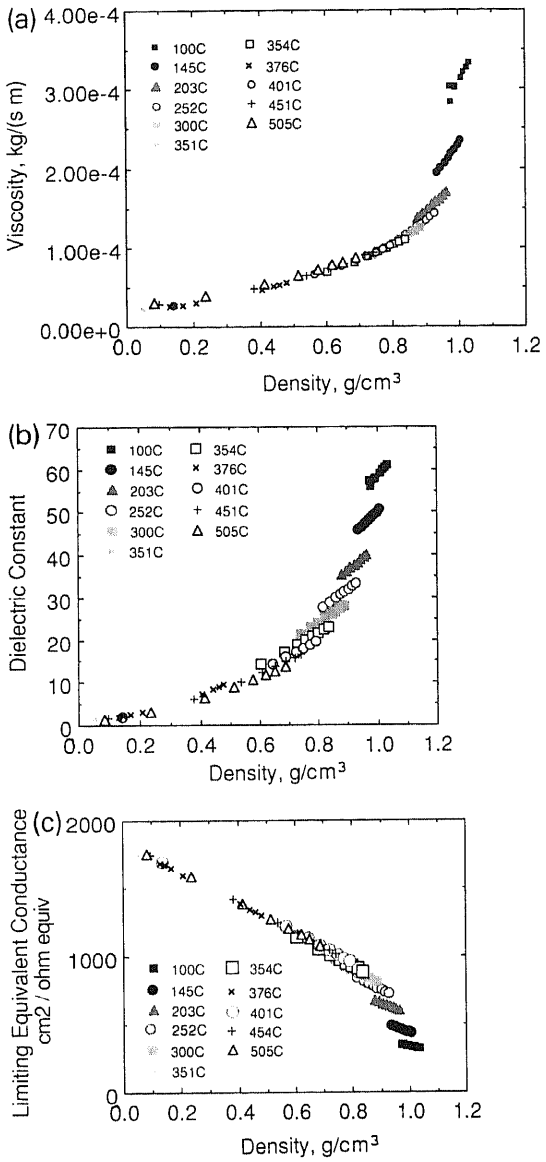

Fig. 11. a. Viscosity of water as a function of density and temperature.b. Dielectric constant of water as a function of density and temperature.c. Limiting equivalent conductance of sodium chloride in water as a function of density and temperature.

the lower-frequency band of the central portion of the envelope, less-structured molecular "associations". The unusually viscous behavior of water under these conditions is most certainly a result of these interactions. As temperature increases, the structure of water appears to simplify with these clusters and molecular associations diminishing in importance. Under these conditions, the viscosity dramatically decreases with increasing temperature. At temperatures of $>250°C$, some clusters appear to persist but the primary spectral feature is a high-frequency band representing relatively unstructured water, which is linear with respect to density and temperature independent at constant density. Under these conditions, viscosity is also primarily dependent on density and nearly independent of temperature. Viscosity is expected to mainly be controlled by water involved in the lowest molecular interaction energy: this explains why similar behavior is observed for viscosity and ν_{max} as a function of temperature and density.

The dielectric constant of water is another bulk property which is sensitive to intermolecular interactions. The dielectric constant is a measure of the ability of the molecules with permanent and/or induced dipoles to orient themselves in an external electric field creating an internal field counter to the externally applied field. Due to the effects of thermal energy which impedes orientation of the dipoles, the dielectric constant normally decreases with increasing temperature. In accordance with the Kirkwood equation, the presence of intermolecular interactions such as those resulting in clusters of hydrogen-bonded water molecules results in anomalously high values of the dielectric constant. At 25°C and 1 bar, the dipole moments of sulfur dioxide and water are quite similar but due to the existence of hydrogen bonding in the latter, its dielectric constant (78.5) is over six times that of the SO_2 (12.3). As in the case of viscosity, the dielectric constant (Haar et al., 1984) is plotted against the density (Fig. 11b). Again, a striking similarity exists with Fig. 10. The trends are somewhat similar to those of viscosity except that the effects of temperature persist to lower densities. This would be expected as the water molecules in clusters exhibit a disproportionately large influence on the dielectric constant. This is not the case with respect to viscosity. The disap-

pearance of clusters and other molecular associations, as discussed above (p.20) is in accord with the rapid decrease of the dielectric constant from 100° to 300°C. The less dramatic but continued decrease with temperature (above 300°C) at constant densities down to 0.4 g cm^{-3} is probabily due to: (1) continued decrease in molecular interactions (the existence of intermolecular associations has an extremely large effect on the bulk dielectric constant); and (2) increasing thermal energy. As in the case of viscosity, a direct correspondence is seen between the spectral evolution of water as a function of temperature and density and a bulk transport property such as the dielectric constant.

The limiting equivalent conductance, a measure of ionic mobility (at infinite dilution) in an external electric field, is plotted for sodium chloride in water (Marshall, 1987) as a function of temperature and density of pure water. Again, large changes occur at temperatures <300°C; above the property becomes linear with density and independent of temperature. The limiting equivalent conductance (A) is proportional to the electric field force (F) and the conventional ionic mobilities if the ions (u_i):

$$A^0 = F(u^0_{\text{conv}+} + u^0_{\text{conv}-}) \quad (1)$$

The conventional ionic mobilities are in turn inversely proportional to the viscosity, η:

$$u^0_{\text{conv}} = z_i e_0 / 1800\pi\rho_i\eta \quad (2)$$

where $z_i e_0$ and r_i are the ionic charge and ionic radius, respectively. It is thus not surprising that the plot of the limiting equivalent conductance of sodium chloride in aqueous solution as a function of temperature and density parallels that of the viscosity (Fig. 11a) and also can be directly correlated to the spectral changes of water (Fig. 10). Since diffusion coefficients ($D^{\pm}$) for a salt can be related to equivalent conductances by the Nernst–Einstein equation:

$$A = zF^2(D^+ + D^-)/RT \quad (3)$$

the simplicity of the relationships of the parameters shown in Figs. 10a and 11a and c as functions of temperature and density allow for the possibility for meaningful theoretical predictions of diffusion coefficients for electrolytes particularly at the lower concentrations ($<1\ m$). The anomolously high value of the limiting equivalent conductance of the hydrogen ion at temperatures <300°C (Marshall, 1987) is another indicator of significant intermolecular hydrogen bonding at temperatures up to almost 300°C. For liquid-like densities, hydrogen ions combine with water molecules forming H_3O^+ complexes. At temperatures and densities at which significant intermolecular associations exist, the protons are able to jump from one molecule to another with enhanced mobility. This anomolous mobility appears to disappear by 300°C with the disappearance of intermolecular connectivity.

4. Discussion

The structure of liquid water has been the subject of numerous investigations and remains controversial (Eisenberg and Kauzmann, 1969; Ben-Naim, 1974). Though oversimplified, Stanley and Teixeira (1980) suggested that the proposed models can be classified as belonging to either: (a) the mixture/interstitial or (b) the distorted hydrogen bond (continuum) categories. In the former, liquid water is assumed to be a mixture of ice-like components and what is termed "normal water" (e.g., Nemethy and Scheraga, 1962). Different and discrete combinations of hydrogen-bonded molecules are assumed to coexist as evidenced by the existence of an isosbestic point (Walrafen, 1967; Walrafen et al., 1986). In the second category, water is thought to ex-

ist as a continuous network of molecules interconnected by somewhat distorted hydrogen bonds (Ratcliffe and Irish, 1982; Rull and Saja, 1986; Sokolowska and Kecki, 1986; Zhelyaskov et al., 1988; Sokolowska, 1989; Efimov, 1990). Molecular dynamics calculations (Geiger et al., 1979; Stillinger, 1980) have supported Frank and Wen's (1957) proposal of the cooperative nature of hydrogen bonding. A hydrogen bond modifies the charge distribution in water molecules in such a way that the hydrogen-bonded molecules are more likely to form additional hydrogen bonds than unbonded molecules. This mutual reinforcement results at low temperatures ($<50°C$) in the formation of a random three-dimensional network of hydrogen-bonded water molecules with local tetrahedral symmetry over that of "iceberg"-like clusters suspended in a sea of unbonded molecules. A statistical approach using percolation theory has been developed to describe this connectivity of water molecules (Geiger et al., 1979; Stanley and Teixeira, 1980). Such studies, which consider only linear hydrogen bonds, predict that a single cluster of doubly-bonded molecules of infinite size does not exist at temperatures above 70° or 80°C. As temperature increases, the network composed of doubly-bonded water molecules becomes increasingly disrupted and fragmented by kinetic effects although local environments of tetrahedral orientation may continue to exist (Dore, 1991). Narten et al. (1967) and Gorbaty and Demianets (1983) have demonstrated the existence of tetrahedrally-coordinated water structures to temperatures of 200°C. Giguère (1984) suggested the existence of a second type of bond, the birfurcated (or bent) hydrogen bond, which may result in weaker network connectivity persisting to higher temperatures than in the case of networks consisting of only linear bonds.

The data collected in this study appear to be in accordance with the continuum models which postulate some form of network connectivity with local tetrahedral symmetry due to linear hydrogen bonding. The frequency of the low-frequency shoulder as monitored by D_2 at 3265 cm^{-1} appears not to change as a function of temperature and pressure and probably represents O–H oscillators in tetrahedrally-coordinated water clusters linked by two linear hydrogen bonds. Green et al. (1986, 1987) and Hare and Sorensen (1990a, b, 1992) demonstrated that in the supercooled region both the intensity and frequency of this low wavenumber band continuously shift toward values of amorphous ice as temperature approaches the singular temperature (−46°C). The higher-frequency portion of the spectral envelope appears to be comprised of two principal components: the low-frequency component located just above 3400 cm^{-1} which appears to predominate at temperatures below 200°C; and the higher-frequency component located above 3550 cm^{-1} which predominates at temperatures of $\geqslant 200°C$. As in the case of the band denoted by D_2 at 3265 cm^{-1}, the low-frequency component also may suggest network connectivity of water molecules but with lower symmetry involving fewer linear (or possibly bent or birfurcated) hydrogen bonds. The high-frequency component is thought to represent O–H oscillators of water molecules free of the direct influence of hydrogen bonding. This suggestion is indicated by the independence of the frequency of the band above 3550 cm^{-1} with respect to temperature at constant density at temperatures above 250–300°C and the linearity of ν_{max} with respect to both liquid-like and vapor-like densities. With increasing temperature and decreasing density, the three-dimensional network of hydrogen bonds weakens with the corresponding decrease of both the prevalence of the local "tetrahedral" structures with double linear hydrogen-bonded water molecules (as denoted by the decrease in intensity of the 3265 cm^{-1} band) and a less symmetric network (as denoted by the decrease in the lower-frequency component of the high-frequency portion of the envelope) with fewer linear (or bent) hydrogen bonds. Con-

sidering the cooperative nature of hydrogen bonding (Frank and Wen, 1957), the decrease in intensity of both of these bands is in all probability interrelated. The high-frequency band has been classically assigned to "free" OH oscillators, i.e. non or weakly hydrogen-bonded oscillators (Walrafen, 1967, 1972; Monosmith and Walrafen, 1984; Giguère and Pigeon-Gosselin, 1986; Sastry and Singh, 1987; Zhelyaskov et al., 1989; Georgiev et al., 1990) but was recently interpreted to result from splitting of the O–H stretching mode due to intermolecular coupling (Hare and Sorensen, 1992). Its disappearance above 200°C may be further indication of the decrease in connectivity with increasing temperature. The increasing simplification of the bulk properties of water (such as the viscosity and dielectric constant) with increasing temperature and decreasing density is a direct result of the increasing dominance of non-hydrogen-bonded molecules at temperatures of >250°C (as evidenced by the band above 3550 cm^{-1}).

Geochemical modelling of supercritical fluids should be approached from the perspective that water under hydrothermal conditions does not exhibit the unusual properties with which it is associated at lower temperatures and pressures. Solubilities, solute complexing, activity coefficients, solvation and diffusion coefficients can be expected to be modelled in a much simpler manner than one is accustomed to at lower temperatures and pressures.

Acknowledgements

This study was jointly supported by the Carnegie Institution of Washington, the Centre National de la Recherche Scientifique and funding from NATO (to J.D.).

References

Benedict, W.S., Gailar, N. and Plyler, E.K., 1956. Rotation–vibration spectra of deuterated water vapor. J. Chem. Phys., 24(6): 1139–1165.

Ben-Naim, A., 1974. Water and Aqueous Solutions — Introduction to a Molecular Theory. Plenum, New York, N.Y., 474 pp.

Bribes, J.L., Gaufrès, R., Monan, M., Lapp, M. and Penney, C.M., 1976. Raman band contours for water vapor as a function of temperature. Appl. Phys. Lett., 28(6): 336–337.

Brooker, M.H., Hancock, G., Rice, B.C. and Shapter, J., 1989. Raman frequency and intensity studies of liquid H_2O, $H_2{}^{18}O$ and D_2O. J. Raman Spectrosc., 20(10): 683–690.

Buback, M., 1981. Spectroscopic investigations of fluids. In: D.T. Rickard and F.E. Wickman (Editors), Chemistry and Geochemistry of Solutions at High Temperatures and Pressures. Pergamon, Oxford, pp. 345–360.

Buldakova, M.A., Matrosov, I.I. and Popova, T.N., 1986. Raman spectra of small water clusters. Zh. Prikl. Spektrosk. 44(1): 54–59 [in Russian; translated into English: J. Appl. Spectrosc., 44(1): 42–45].

Dawson, B.S.W., Irish, D.E. and Toogood, G.E., 1986. Vibrational spectral studies of solutions at elevated temperatures and pressures, 8. A Raman spectral study of ammonium hydrogen sulfate solutions and the HSO_4^-–SO_4^{2-} equilibrium. J. Phys. Chem., 90: 334–341.

Dore, J.C., 1991. Structural studies of water and other hydrogen-bonded liquids by neutron diffraction. J. Mol. Struct., 250: 193-211.

Efimov, Y.Y., 1990. Ensembles of hydrogen bonds in liquids, ice nuclei, and in computer modeling. J. Mol. Struct., 237: 93–103.

Eisenberg, D. and Kauzman, W., 1969. The Structure and Properties of Water. Oxford University Press, New York, N.Y., 282 pp.

Engdahl, A. and Nelander, B., 1989. Water in krypton matrices. J. Mol. Struct., 193: 101–109.

Falk, M., 1990. Frequencies of H–O–H, H–O–D and D–O–D bending fundamentals in liquid water. J. Raman Spectrosc., 21: 563–567.

Franck, E.U. and Roth, K., 1967. Infrared absorption of HDO in water at high pressures and temperatures. Discuss. Faraday Soc., 43: 108–114.

Frank, H.S. and Wen, W., 1957. Ion–solvent interaction, III. Structural aspects of ion–solvent interaction in aqueous solutions: a suggested picture of water structure. Discuss. Faraday Soc., 24-26: 133–140.

Geiger, A., Stillinger, F.H. and Rahman, A., 1979. Aspects of the percolation process for hydrogen-bond networks in water. J. Chem. Phys., 70(9): 4185–4193.

Georgiev, G.M., Nickolov, Z.S., Zhelyaskov, V.R. and Miteva, M.I., 1990. Raman study of the "free" OH groups in H_2O- mixtures using Fourier deconvolution technique. J. Mol. Struct., 45: 45–48.

Giguère, P.A., 1984. Bifurcated hydrogen bonds in water. J. Raman Spectrosc., 15(5): 354–359

Giguère, P.A. and Pigeon-Gosselin, M., 1986. The nature

of the "free" OH groups in water. J. Raman Spectrosc., 17(4): 341–344.

Gorbaty, Y.E. and Demaniets, Y.N., 1983. The pair-correlation functions of water at a pressure of 1000 bar in the temperature range 25–500°C. Chem. Phys. Lett., 100(5): 450–454.

Green, J.L., Lacey, A.R. and Sceats, M.G., 1986. Spectroscopic evidence for spatial correlations of hydrogen bonds in liquid water. J. Phys. Chem., 90(17): 3958–3964.

Green, J.L., Lacey, A.R., Sceats, M.G., Henderson, S.G. and Speedy, R.J., 1987. Coupling of small-amplitude proton motions in liquid water to density and temperature. J. Phys. Chem., 91(6): 1684–1686.

Haar, L., Gallagher, J.S. and Kell, G.S., 1984. Steam Tables: Thermodynamic and Transport Properties and Computer Programs for Vapor and Liquid States of Water in SI Units. NBS/NRC — National Standard Reference Data System. Hemisphere, New York, N.Y., 320 pp.

Hadidiacos, C.G., 1977. Linear programmable temperature controller. Carnegie Inst. Washington Yearbk., 76: 664–668.

Hare, D.E. and Sorensen, C.M., 1990a. Raman spectroscopic study of bulk water supercooled to −33°C. J. Chem. Phys., 93(1): 25–33.

Hare, D.E. and Sorensen, C.M., 1990b. Raman spectroscopic study of dilute HOD in liquid H_2O in the temperature range −31.5 to 160°C. J. Chem. Phys., 93(10): 6954–6961.

Hare, D.E. and Sorensen, C.M., 1992. Interoscillator coupling effects on the OH stretching band of liquid water. J. Chem. Phys., 96(1): 13–22.

Herzberg, G., 1968. Molecular Spectra and Molecular Structure, II. Infrared and Raman Spectra. Van Nostrand, London, 632 pp.

Irish, D.E., McCarroll, B. and Young, T.F., 1963. Raman study of zinc chloride solutions. J. Phys. Chem., 39(12): 3436–3444.

Kohl, W., Lindner, H.A. and Franck, E.U., 1991. Raman spectra of water to 400°C and 3000 bar. Ber. Bunsenges. Phys. Chem., 95: 1586–1593.

Lindner, H.A., 1970. Ramanspektroskopische Untersuchungen an HDO, gelöst in H_2O, an HDO in wässerigen Kaliumjodidlösungen und an reinem H_2O bis 400°C und 5000 bar. Ph.D. Thesis, Universität Karlsruhe, Karlsruhe, 81 pp.

Ludeman, H.D. and Franck, E.U., 1967. Absorptionspektren bei hohen Drücken und Temperaturen, I. Wässerige Co(II) und Ni(II)-Halogenid-Lösungen bei 500°C und 6 kbar. Ber. Bunsenges. Phys. Chem., 71: 455–460.

Ludemann, H.D. and Franck, E.U., 1968. Absorptionspektren bei hohen Drücken und Temperaturen, II. Kobalt(II) und Nickel(II)-Halogenid-Lösungen. Ber. Bunsenges. Phys. Chem., 72: 514–523.

Marshall, W.L., 1987. Reduced state relationship for limiting electrical conductances of aqueous ions over wide ranges of temperature and pressure. J. Chem. Phys., 87(6): 3639–3643.

Monosmith, W.B. and Walrafen, G.E., 1984. Temperature dependence of the Raman OH-stretching overtone from liquid water. J. Chem. Phys., 81(2): 669–674.

Mysen, B.O., Finger, L.W., Seifert, F.A. and Virgo, D., 1982. Curve fitting of Raman spectra of amorphous materials. Am. Mineral., 67: 686–696.

Narten, A.H., Danford, M.D. and Levy, H.A., 1967. X-ray diffraction study of liquid water in the temperature range 4–200°C. Discuss. Faraday Soc., 42: 97–107.

Nemethy, G. and Scheraga, H.A., 1962. Structure of water and hydrophobic bonding in proteins, I. A model for the thermodynamic properties of liquid water. J. Chem. Phys., 36(12): 3382–3400.

Penney, C.M. and Lapp, M., 1976. Raman-scattering cross sections for water vapor. J. Opt. Soc. Am., 66(5): 422–425.

Ratcliffe, C.I. and Irish, D.E., 1982. Vibrational studies of solutions at elevated temperatures and pressures, 5. Raman studies of liquid water up to 300°C. J. Phys. Chem., 86: 4897–4905.

Rull, F. and de Saja, J.A., 1986. Effect of electrolyte concentration on the Raman spectra of water in aqueous solutions. J. Raman Spectrosc., 17: 167–172.

Sastry, M.I.S. and Singh, S., 1987. Derivative analysis of Raman spectra of liquid water in the O–H(D) stretching region. J. Mol. Struct., 158: 195–204.

Schulz, K.R., 1974. Ramanspektroskopische Untersuchungen an wässerigen Zinkchloridlösungen bis 500°C und 4000 bar. Ph.D. Thesis, Universität Karlsruhe, Karlsruhe, 81 pp.

Seward, T.M., 1984. The formation of lead(II) chloride complexes to 300°C — A spectrophotometric study. Geochim. Cosmochim. Acta, 48: 121–134.

Sokolowska, A., 1989. Effect of temperature on the Fermi resonance and the resonance intermolecular coupling in the Raman spectra of liquid water. J. Raman Spectrosc., 20: 779–783.

Sokolowska, A. and Kecki, Z., 1986. Inter- and intra-molecular coupling and Fermi resonance in the Raman spectra of liquid water. J. Raman Spectrosc., 17: 29–33.

Stanley, H.E. and Teixeira, J., 1980. Interpretation of the unusual behavior of H_2O and D_2O at low temperatures: test of a percolation model. J. Chem. Phys., 73(7): 3404–3422.

Stillinger, F.H., 1980. Water revisited. Science, 209(4455): 451–457.

Stryland, J.C. and Till, S.M., 1977. High-pressure optical cell for Raman scattering studies in solid hydrogen. Rev. Sci. Instrum., 48(10): 1350–1351.

Susak, N.J. and Crerar, D.A., 1985. Spectra and coordination changes of transition metals in hydrothermal

solutions. Implications for ore genesis. Geochim. Cosmochim. Acta, 49: 555–564.

Susak, N.J., Crerar, D.A., Forseman, T.C. and Hass, J.L., 1981. Improved spectrophotometric cell for hydrothermal solutions. Rev. Sci. Instrum., 52(3): 428–431.

Thiel, M.V., Becker, E.D. and Pimentel, G.C., 1957. Infrared studies of hydrogen bonding of water by the matrix isolation technique. J. Chem. Phys., 27(2): 486–490.

Tursi, A.J. and Nixon, E.R., 1970. Matrix-isolation study of the water dimer in solid nitrogen. J. Chem. Phys., 52(3): 1521–1528.

Valyashko, V.M., Buback, M. and Franck, E.U., 1980. Infrared absorption of concentrated aqueous LiCl solutions to high pressures and temperatures. Z. Naturforsch., 35a: 549–555.

Van Thiel, M., Becker, E.D. and Pimentel, G.C., 1957. Infrared studies of hydrogen bonding of water by the matrix isolation technique. J. Chem. Phys., 27(2): 486–490.

Walrafen, G.E., 1967. Raman spectral studies of the effects of temperature on water structure. J. Chem. Phys., 47: 114–126.

Walrafen, G.E., 1972. Raman and infrared spectral investigations of water structure. In: F. Franks (Editor), Water — A Comprehensive Treatise. Plenum, New York, N.Y., pp. 151–214.

Walrafen, G.E., Fisher, M.R., Hokmabadi, M.S. and Yang, W.H., 1986. Temperature dependence of the low- and high-frequency Raman scattering from liquid water. J. Chem. Phys., 85(12): 6970–6982.

Whalley, E., Klug, D.D. and Handa, Y.P., 1991. Some aspects of hydrogen bonding in the phases of water. J. Mol. Struct., 250: 337–349.

Zhelyaskov, V., Georgiev, G. and Nickolov, Z., 1988. Temperature study of intra- and inter-molecular coupling and Fermi resonance constants in the Raman spectra of liquid water using Fourier deconvolution. J. Raman Spectrosc., 19: 405–412.

Zhelyaskov, V., Georgiev, G., Nickolov, Z. and Miteva, M., 1989. Concentration (D_2O in H_2O) and temperature Raman study of the molecular interactions in the OD stretching spectra of D_2O and D_2O/H_2O mixtures using the Fourier deconvolution technique. J. Raman Spectrosc., 20(2): 67–75.